Experimental Study on the Mechanical Effects of the Vibration-Assisted Ball-Burnishing Process

Jose Antonio Travieso-Rodríguez, Giovanni Gomez-Gras, Jordi Jorba-Peiro, Francisco Carrillo, Gilles Dessein, Joël Alexis, Hernan Alberto González-Rojas

Experimental Study on the Mechanical Effects of the Vibration-Assisted Ball-Burnishing Process

J. A. Travieso-Rodriguez[1], G. Gómez Gras[1], J. Jorba Peiró[1], F. Carrillo[2], G. Dessein[2], J. Alexis[2], and H. González Rojas[1]

[1]*Escola Universitaria d'Enginyeria Tècnica Industrial de Barcelona (EUETIB), Departament d'Enginyeria Mecànica, Universitat Politècnica de Catalunya,*
[2]*École National d'Ingénieurs de Tarbes, Laboratoire Génie de Production, Université de Toulouse,*

Burnishing processes are effective methods for treating pieces to increase their durability and roughness. Studies reveal that traditional burnishing can be strongly improved with the assistance of external energy sources. A vibrating module was attached to a classical burnishing tool and was tested on aluminum specimens to find the optimal vibration-assisted burnishing parameters. Vibration caused roughness improvements of the specimens and decreased the processing time by fivefold compared to traditional burnishing. At the tested frequency, no significant consequences were found on hardness and residual stresses.

Keywords Aluminum; Burnishing; Hardness; Manufacturing; Residual; Roughness; Stress; Vibration.

Introduction

Current industry demands mechanical components with a high fatigue resistance and low friction ratio. This demand grows larger with the necessity of the manufacturing components requiring compressive residual stress in deep layers, high hardness and low surface roughness.

These specifications can be obtained through several processes, including burnishing, blast shot peening and electropolishing. Shepard et al. [1] analyzed the response to fatigue of pieces from the aeronautical industry manufactured with Ti-6Al-4V. These pieces were submitted to three processes: ball-burnishing, blast shot peening and electropolishing, and a comparative analysis of their surface roughness and compressive residual stress was performed. The highest roughness was achieved in the ball-burnished parts (average roughness $R_a \approx 3\,\mu m$), while electropolishing and peening resulted in $R_a \approx 17\,\mu m$ and $R_a \approx 85\,\mu m$, respectively.

Ball-burnishing is considered a cold-working process, according to Yen [2]. It is developed using a tool attached to a machine head, applying a certain calibrated force to a sphere. This sphere glides over the workpiece area, deforming the peaks of surface irregularities and flattening the surface profile, producing a much more regular surface. During the process, elastic-plastic deformation is produced on the workpiece surface because the tool is constantly impacting on it [3–5], increasing the superficial hardness and introducing compressive residual stress in the most superficial levels of the material.

Many ball-burnishing tools exist on the market. Some of them develop their function through a spring that transmits the force to the burnishing ball. Several authors have used this type of tool in the development of their research, as noted by Hassan et al. [6] and El-Axir et al. [7]. In other tools, the force applied to the ball is originated by a hydraulic system through the circulation of a pressured fluid. This tool has been presented by Travieso-Rodríguez et al. [8] and is commercialized by the following companies: Mech-India Engineers [9] and Ecoroll AG Werkzeugtechnik [10].

Using both types of tools, numerous investigations have shown the effects of burnishing. Celaya et al. 11] published a model of the burnishing process, with outputs in surface finishing and residual stresses on mechanical parts. This model was used to study the effects of two parameters (feed and fluid pomp pressure) on the process. Rodriguez et al. [12] analyzed the behavior of this operation in a turning process, comparing the surface results of pieces mechanized through a turning operation and others finished through to ball-burnishing. Surface roughness, hardness and compressive residual stresses were analyzed. Burnishing caused R_a up to 0.3 μm, an increase of 60% in hardness, and residual stresses of approximately −350 MPa. As shown in referenced papers, this process has also been studied and evaluated by our group. We have shown the influence of burnishing on surface finishing, hardness and changes in the compressive stress map.

The compressive force involved in the burnishing process is crucial for obtaining positive results. The material deformation is constrained by a certain limit determined by its properties, so acting on these during

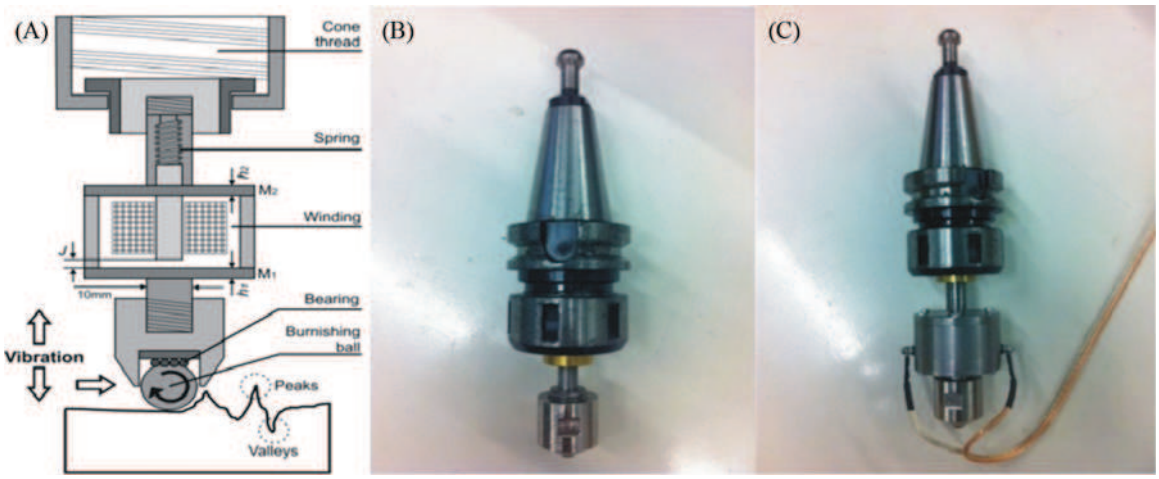

FIGURE 1.—Tools used in the experiments. A- Functional diagram of the vibration system. M_1: Plate attached to the burnishing ball, M_2: Plate attached to the spring, h_1: M_1 plate thickness, h_2: M_2 plate thickness, J: Gap. B- Tool assembled for the non-vibration-assisted process, C- Tool assembled for the vibration-assisted process. Parameter values: $h_1 = h_2 = 2$ mm, $J \geq 3$ mm [16].

the burnishing process is necessary to attain better results. An alternative method to modify the way the material is deformed during the burnishing process is assisting with a vibrational source. Vibration helps in increasing the velocity with which dislocations move and allows a better internal restructuring of the material's microstructure while it is deforming [13, 14]. These considerations lead us to believe that a vibration-assisted ball-burnishing process (VABB) is comparable to a conventional process and justifies the study presented in this paper. Furthermore, we have found nothing in the literature that has shown the existence of vibration-assisted burnishing tools.

The following hypotheses are addressed in this study:

1. Are the values of surface roughness affected by vibrations in a burnishing process?
2. Does the VABB process increase the superficial hardness of workpieces compared to the values obtained by the conventional burnishing process?
3. Does the VABB change the compressive residual stress map in the external layers of the material, achieving higher values at deeper levels compared to values obtained through the conventional burnishing process?

The principal objective and innovative scope of this paper is to study the mechanical effects of the VABB process on burnished workpieces.

To perform this study, a vibrating burnishing tool was manufactured and patented by Travieso-Rodriguez et al. [15], as shown in Fig. 1-A. The tool can be easily installed using an ISO cone (Figs. 1-B and 1-C) in the same CNC machine where the piece was previously machined. Inside the tool body (Fig. 1-A), a spring is used to provoke a constant burnishing force. Another oscillating force, originating from the vibration of the burnishing ball, is added to the system. This force is a result of the existing magnetic field induced by a coil on a metal core attached to the tool. The coil is inside a cylinder closed on both faces using two plates, M_1 and M_2. These plates are coupled and adjusted to a default working frequency, transmitting their movement to the bottom of the tool where the ball burnishing is performed. The ball is in contact with a bearing, which facilitates its free rotational movement. The bearing is formed by several spheres with a 2 mm diameter. Plastic deformation of the workpiece is produced by a hard ball with a 10 mm diameter. This tool was manufactured by assembling different modules so that the vibrating coil can be detached from the rest of the tool. This allows for burnishing with or without vibrational assistance (Figs. 1-B & 1-C, respectively).

Different burnishing experiments were carried out using the described tool, and an evaluation of surface hardness, residual stress and surface roughness quality indicators (dependent variables) were analyzed. These results were compared with conventionally burnished pieces. The response surface DOE is used to define the experimental strategy. The results derived from the measurement of each evaluated parameter are presented, and recommended parameters for the use of this technology are summarized.

MATERIALS AND METHODS

Different experiments were performed on workpieces of aluminum A92017-T4 (Fig. 2). Aluminum pieces were machined in a CNC milling machine using an 8 mm diameter mill, cutting speed of 3000 min^{-1}, feed rate of 1380 mm/min and 0.5 mm depth of cut (Fig. 2-A). The milling operation was carried out in successive parallel passes in steps of 2 mm. Two pieces were mechanized, as shown in Fig. 2-A, and each of them were submitted to a burnishing operation, as shown in Fig. 2-B. The first piece was submitted to a conventional burnishing

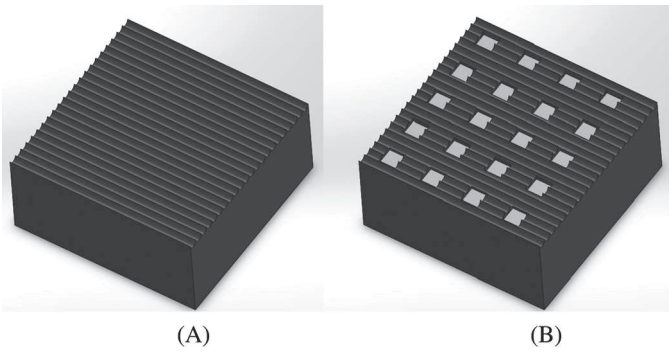

FIGURE 2.—Workpieces used for testing the surface roughness. A- after milling. B- after burnishing.

process, and the second piece was submitted to a burnishing process in the presence of vibration.

To carry out burnishing operations, three parameters were evaluated: burnishing force F (related to the pre-load that adjusts the tool), the feed rate of the tool f and the number of passes n. In operations consisting of more than one pass, successive paths were always performed after previous ones. The tool worked with 2500 Hz frequency, coincident with the first natural frequency of the system. Its amplitude was 0.0013 mm. Other processing parameters were kept constant, including the burnishing strategy (at right angles with the first milling operations), the lateral pass width b of 0.08 mm and the ball diameter of 10 mm. To determine these parameters, values from the literature [17] were taken into account.During the experiments, the values of the forces have been measured by placing the workpieces on a dynamometer Kirstler model 9257B, so that the process can be monitored in real time, and allowing keeping a record of the force values applied in all the experiments. Sampling frequency was 10Kz, and data was obtained for one minute during the experiment.

Three measures were used to evaluate the quality of the piece after being subjected to the described process: surface roughness, hardness and residual stress.

The study of toughness was developed through 23 experimental designs obtained through the combination of the parameters mentioned in the previous paragraph. This resulted in eight combinations with two replicates and four central points, which produced a total of twenty different surfaces in each piece. Each burnishing operation was carried out either with or without vibrational assistance. Surface roughness was characterized by two indicators based on R_a (average surface roughness, i.e., R_a in the parallel direction of the burnishing tool feed rate ($R_a//$) and in the perpendicular direction of the burnishing tool feed rate ($R_a\perp$)).

The hardness profile from the surface of the workpiece to its inner layers was evaluated to understand the effect of vibrations during the burnishing process on the superficial hardening of the material. Measures of hardness were executed on a surface right-angled to the burnished surface. The specimens were mounted in Bakelite, grinded and polished, according to usual procedures for metallographic analysis. The Vickers Hardness was determined at five points on specimens burnished with and without vibrational assistance by a microdurometre Buehler 5114, applying a force of 0.029N for 10 s. A 2 mm depth was tested starting from the burnished surface, and prints were adequately distributed to comply with ISO 6507 standards.

Residual stresses on the surface were measured before and after vibration-assisted and non-vibration-assisted burnishing. Stresses were calculated using the $\sin^2\Psi$ method, according to Noyan et al. [18], and based on the fact that the distance between the same type of crystalline planes of certain material, d, is a consequence of the residual stress stored in that material. The change in the interplanar spacing (d_Ψ) along the inclined angle of the specimen (Ψ) for the same incidence angle (θ) was calculated from the displacement of the diffraction peaks obtained through a Ψ-mode (Fig. 3A). Measurements were performed in a Panalytical X Pert PRO diffractometer with a position sensitive detector (PSD) configured in scan mode between 113.50 and 119.50 of the diffraction angle 2θ that corresponded to {420} crystallographic planes of aluminum using Co-Ni filtered X-ray radiation corresponding to a wavelength of 0.15406 nm. Measurements were taken directly on the surface of specimens, keeping the illuminated area constant. The value for residual stress (σ_φ) under each burnishing condition was calculated from the experimental values adjusted to Eq. 1.

$$\frac{d_\psi - d_0}{d_0} = \frac{1+\nu}{E}\cdot\sigma_\phi\cdot\frac{1}{\sin^2\psi} - \frac{\nu}{E}(\sigma_{11}+\sigma_{22}) \qquad (1)$$

Where E is the Young's modulus and ν is Poisson's ratio; σ_{11} y and σ_{22} are the normal stresses on a flat stress state of the target area of material; and d_o the interplanar distance for inclination angle of the specimen $\Psi = 0$.

Figure 3-A shows the displacement of the diffraction peaks for the planes {420} depending on the residual stress for one of the analyzed conditions. Figure 3-B shows a regression line of the experimental values for a vibration-assisted-burnished specimen. The reported values of residual stress have been calculated from the slope of the line adjusted to Eq. 1, taking the following values for E = 69.204 GPa and $\nu = 0.358$, based on the information given by Hauk et al. [19]. Many metallic specimens absorb X-rays proportionally to the distance travelled into the material from the surface to deeper planes where diffraction occurs, with the x-rays being detected after returning to the surface. For this reason, the effective penetration depth is usually defined as the center of gravity of the measured diffracted distribution intensity versus depth for an infinitely thick, homogenous specimen and is dependent upon the incident and exit angles of incoming and diffracted X-rays. The values reported in this paper are the average of residual stresses acting in a volume confined by a specific depth below the sample surface that originates approximately

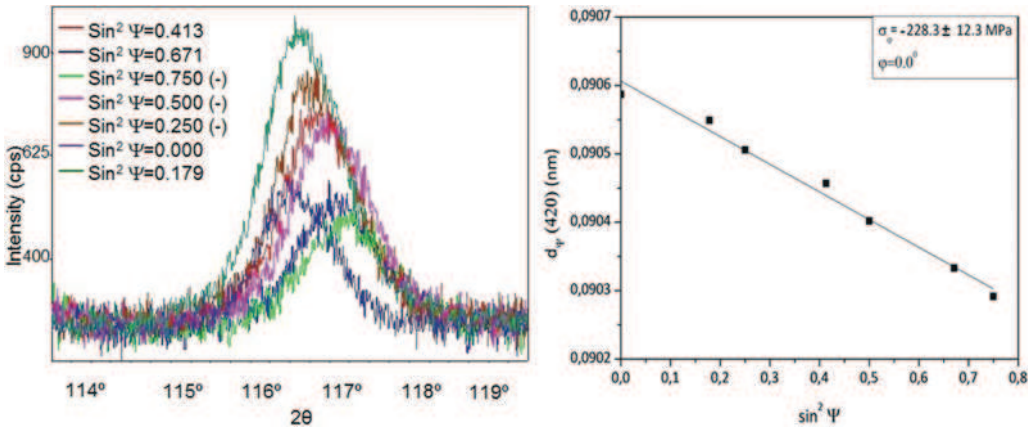

FIGURE 3.—A- Variation of the diffraction angle (2θ) based on the incidence angle (Ψ). B- Variation of the interplanar distance of {420} planes depending on $\sin^2\Psi$.

63% of the diffracted intensity, according to Kumar et al. [20].

RESULTS AND DISCUSSION

Table 1 shows the values of the measured surface roughness, which improved for all burnished specimens compared to specimens submitted to a previous milling operation without subsequent processing. Non-vibration-assisted-burnished (NVABB) specimens experienced a 54% improvement in R_a along the parallel direction of the burnishing path and 57% improvement in the perpendicular direction. Vibration-assisted burnishing increased R_a by 64% in the parallel direction and increased R_a by 92% in perpendicular measurements. Vibration-assisted burnishing results in a better roughness of 80% for $R_a\perp$ and 20% for the $R_a//$ parameters.

TABLE 1.— Results of surface roughness measurements.

				Non-vibration-assisted		Vibration-assisted	
Experiment	F (N)	f (mm/min)	n	$R_a\perp$	$R_a//$	$R_a\perp$	$R_a//$
1	110	600	5	0.70	2.61	0.16	0.91
2	110	600	5	0.81	2.69	0.15	1.47
3	110	600	1	1.40	3.90	0.22	3.21
4	110	600	1	0.68	3.87	0.25	3.45
5	110	400	5	0.86	2.12	0.18	1.62
6	110	400	5	1.16	2.25	0.16	2.11
7	110	400	1	1.70	4.26	0.22	3.02
8	110	400	1	0.57	3.81	0.21	3.58
9	105	500	3	0.48	3.07	0.14	1.67
10	105	500	3	0.79	2.85	0.16	1.93
11	105	500	3	0.30	3.74	0.15	2.22
12	105	500	3	1.22	3.47	0.18	2.75
13	100	600	5	0.47	3.82	0.14	3.13
14	100	600	5	0.30	2.82	0.14	2.76
15	100	600	1	1.18	3.99	0.18	3.57
16	100	600	1	1.74	4.33	0.17	4.31
17	100	400	5	0.46	3.51	0.14	2.94
18	100	400	5	0.40	3.03	0.13	2.83
19	100	400	1	0.59	4.40	0.21	3.34
20	100	400	1	1.47	3.87	0.18	4.03
Previous milling				2.02	7.51	2.06	7.62

Previous milling and burnishing processes have been carried out at right angles. This fact explains the difference between roughness values obtained for different-measured paths. Analyses were based on a Pareto chart, as shown in Fig. 4, where the most significant parameters are represented, taking into account a 95% confidence level. The most important variable to control was the number of passes (n), as it was statistically significant in all experiments. Compression force was also important in all experiments, except for measurements along the perpendicular direction in non-vibrating-assisted burnishing. Trends were similar for every parameter in each case, but the conditions applied in experiment A, Fig. 4, were the least significant. The feed parameter, f, was not relevant in any of the studied conditions.

It is also important to consider the influence of the combination of processing parameters (f, F and n) on the final R_a. Figure 5 shows graphics used for this analysis. In Fig. 5-A, $R_a//$ values measured in burnished specimens with just one pass are represented. Figure 5-B shows burnished specimens after five passes. Figures 5-C and 5-D show similar results for the values of roughness $R_a\perp$ measured in the perpendicular direction. These figures show that when using vibration-assisted burnishing, comparable results are obtained for one and five passes. Performing the procedure in one pass is desirable and would save a considerable amount of time. This fact is more noticeable in Fig. 5-E, where the results are compared between those achieved with conventional burnishing with five passes and with vibration-assisted burnishing in one pass for the same operational parameters (f, F and n). Furthermore, burnishing in just one pass with vibrational assistance strongly decreases the dispersion of measured values. Changes in the advance speed of the tool in its values do not affect substantially the value of dispersion and roughness.

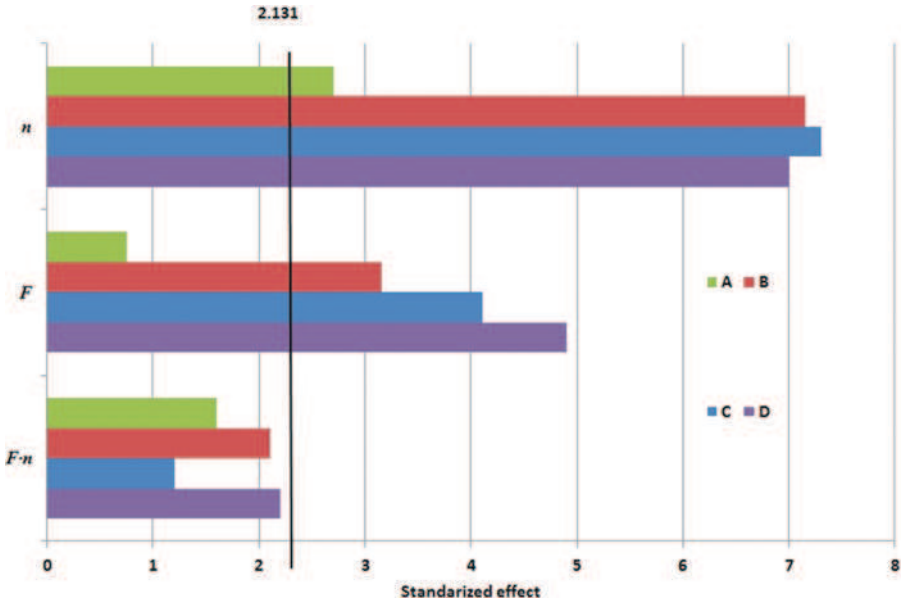

FIGURE 4.—Summary Pareto chart for the standardized effects of different system variables on aluminum A-92017 workpieces. A- $R_a\perp$ non vibration-assisted burnishing. B- $R_a//$ non vibration-assisted burnishing. C- $R_a\perp$ vibration-assisted burnishing. D- $R_a//$ vibration-assisted burnishing.

Therefore, burnishing with an advance speed of 600 mm/min is desirable to reduce the processing time and increase efficiency.

In light of the hardness measurement results, it can be asserted that the compression force applied with the vibrating system does not affect the hardness profile within the studied range. When the feed and number of passes are kept constant ($f = 400$ mm/min, $n = 1$), the material hardens through a 100 µm deep thickness (Fig. 6-A). This hardening effect increases with an increasing number of passes (Fig. 6-B), but decreases with the increasing feed of the burnishing ball. The hardening effect of the 100 µm deep area of the material is noticeable if the burnishing feed is 400 mm/min with or without vibrations (Fig. 6-C) and also if feeds increase to 600 mm/min with vibrations. However, the same feed without vibrations makes hardening unnoticeable.

This increase in hardness from the surface reached a maximum at approximately 80-100 µm deep planes and then subsequently decreases. This behavior is similar to the compression residual stress acting at the same depth under the surface of 100Cr6 steel (equivalent to UNS G52986) hardened, turned and ball-burnished and is comparable to results published by Yen et al. [21]. On the other hand, no explanation has been found for the hardness profile after non-vibration-assisted ball burnishing using 110N of force, a feed of 600 mm/min and 5 passes (Fig. 6-D). When applying a vibration-assisted process, the profile is similar to other conditions.

Assisting the ball-burnishing process with vibrations, make it more practicable. This phenomenon has been explained by Yin and Shinmura [22]. The effect of the vibrational energy on the surface roughness of the material at least can be explained by two simultaneous mechanisms. The first mechanism is related to the reduction of the friction between the ball which acts as a tool and the surface of the workpiece [23]. This minor friction eases the movement of material in contact with the ball decreasing the final roughness of the surface. The second mechanism is related with the interaction of vibration waves and material which dissipates power that helps to release the anchored dislocations that are in the outermost part of the material layers, as was explained by Holstein [24]. These dislocations once released, would facilitate the plastic deformation of this area of the material or the decrease of the elastic limit [Blaha, 25]. In this way, although the total forces applied on the surface of the material in a VABB and NVABB process are similar; their effect on the material is noted. In fact, the values of the forces applied in both processes, only differ in a range of 5 to 8N for all experiments while the effect on the final roughness decrease clearly when vibration is applied. The both mechanism explain why the results obtained with one pass using VABB process, are the same as with five passes using NVABB.

Residual stress measured for the specimens submitted to different burnishing conditions with and without vibrations assistance are shown in Table 2. These values increase in the burnished areas of the specimens compared to the values obtained in workpieces finished with the milling process [26]. This phenomena is present both in conventional burnishing, where growth is approximately 115% on the initial value, and in VABB, where 365% growth is achieved. Although these values are different compared to milled specimens, there is no significant difference between residual stresses after submitting the specimen to both burnishing operations.

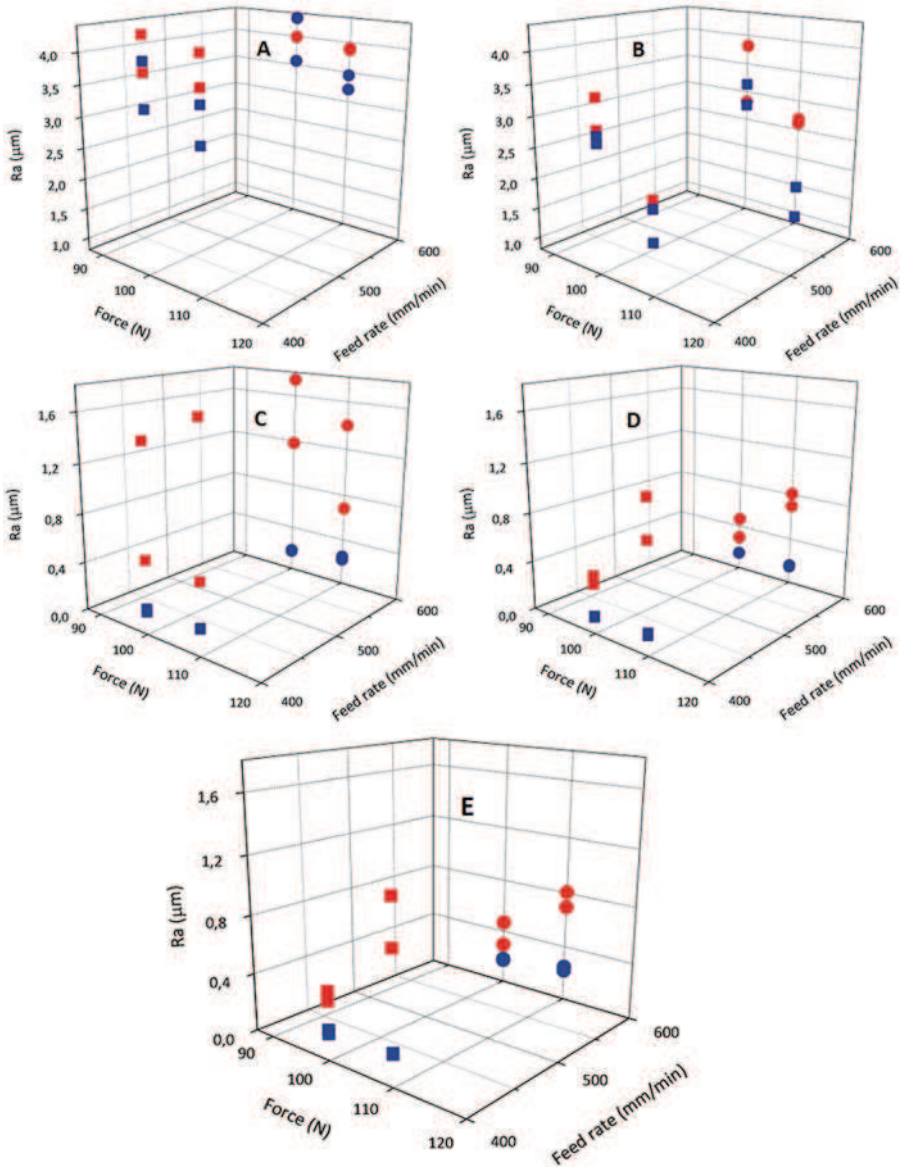

FIGURE 5.—Influence of the parameters on the surface roughness in A92017 workpieces. A- $R_a//$: 1pass. B- $R_a//$: 5passes. C- $R_a\perp$: 1pass. D- $R_a\perp$: 5passes. Blue: vibration-assisted-burnishing; Red: non-vibration-assisted-burnishing; Circles: $f = 600$ mm/min; Squares: $f = 400$ mm/min. E- Comparison between conventional burnishing process and vibration-assisted-burnishing for the same system parameters (f, F and n). Blue: vibration-assisted burnishing, 1pass. Red: non-vibration-assisted burnishing, 5passes.

These results suggest that the initial residual stress distribution did not significantly affect the residual stress produced during ball-burnishing and corroborates the conclusions reached by Roettger [4]. In fact, although the vibrations affect the mobility of dislocations and the friction between the ball and the surface of the material, the degree of deformation of the surface area has probably reached a degree of saturation in which compressive residual stress generated in VABB and NVABB are the same regardless of initial value.

On the other hand, the effective penetration depth of X-ray is approximately 30 µm in the best experimental conditions ($\Psi = 0$), which is very low compared to the 80-100 µm depth for maximum hardness. However, it has been reported that the residual stress profile determined using the deflection-etching technique increased from the surface to a maximum at depths ranging from 100 to 200 µm when an aluminum alloy AA6061-T6 was ball-burnished with no vibration [27].

The experiments performed allow for drawing interesting conclusions about the development of future research directions on VABB processing with tested material. These recommendations for development tool are F = 100N, $f = 600$(mm/min), 1pass, $b = 0.08$ mm, burnishing strategy: Perpendicular to previous milling and Vibration frequency 2500 Hz.

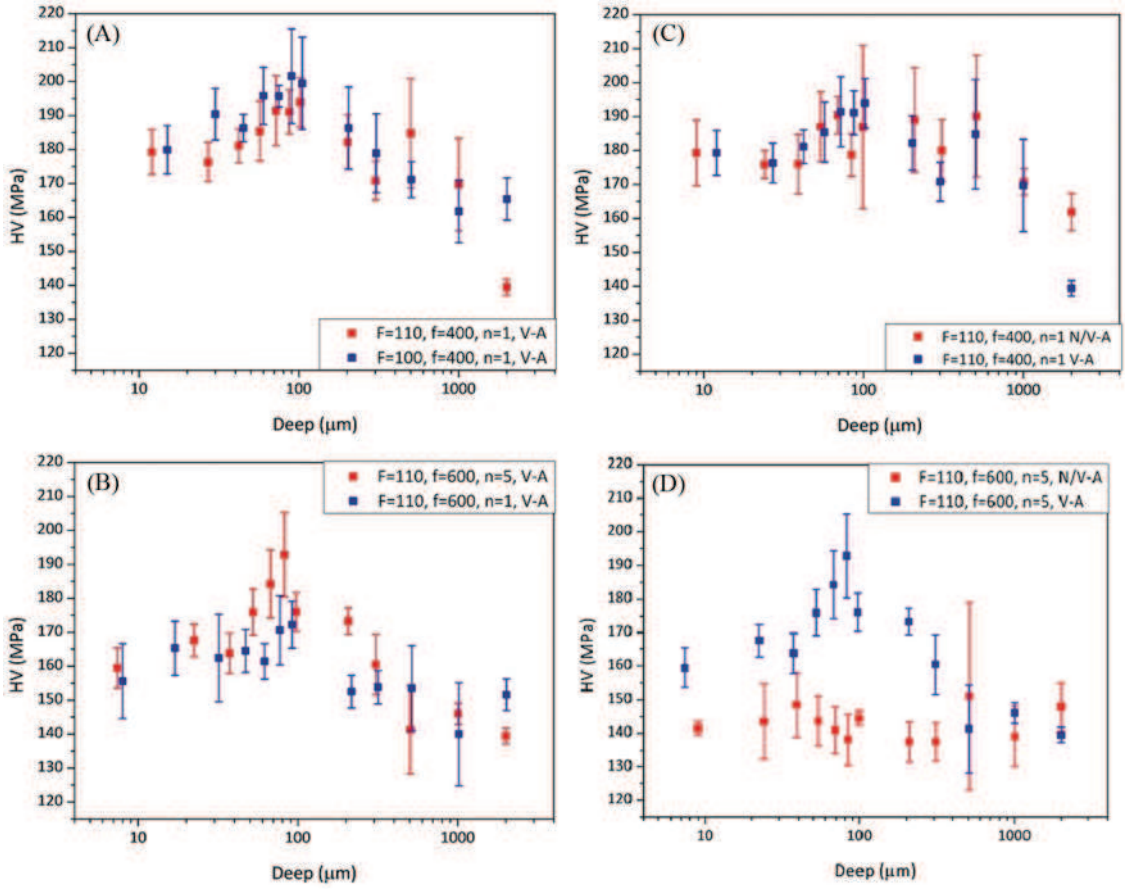

FIGURE 6.—Micro-hardness measured in the workpiece profile obtained with Forces $F_1 = 100$N, $F_2 = 110$N, A- $f = 400$ mm/min and $n = 1$ using vibration. B- $f = 600$ mm/min and $n = 5$ using vibration. C- $f = 400$ mm/min and $n = 1$ with or without vibration. D- $f = 600$ mm/min and $n = 5$ with vibration and without it.

TABLE 2.— Results of residuals stress measurements, σ_φ (MPa).

F (N)	f (mm/min)	n	Non vibration-assisted	Vibration-assisted
110	500	1	-232.5 ± 14.4	-228.3 ± 12.3
105	500	1	-234.9 ± 13.5	-218.8 ± 8.0
Before burnishing			-74.1 ± 10.7	-48.0 ± 3.6

CONCLUSIONS

The results from this study support our hypothesis and conclusion that the effects of a VABB process are substantially different from those derived from a conventional burnishing operation.

1. Average values of $R_a//$ and $R_a\perp$ decrease when a vibration-assisted process is applied.
2. When VABB process is performed, less burnishing passes are required to improve surface roughness. Therefore, the processing time decreased for the range of parameters used in this article.
3. Vibrations do not cause significant changes to hardness profiles for most of the tested conditions. However, hardness increases with an increase in the number of passes in the presence of vibrations.
4. There is no significant difference between the residual stresses obtained through either process that was detectable using the X-ray diffraction method.

ACKNOWLEDGMENTS

Financial support for this study was provided by the Ministry of Economy and Competitiveness of Spain through grant DPI2011-26326 (J-01686) and is greatly appreciated.

REFERENCES

1. Shepard, M.J.; Prevéy, P.S.; Jayaraman, N. Effects of Surface Treatment on Fretting Fatigue Performance of Ti-6Al-4V. In *Proceedings of the 8th National Turbine Engine High Cycle Fatigue Conference*, Monterrey, Mexico, April 14–16, 2003.
2. Yen, Y.C.; Sartkulvanich, P.; Altan, T. Finite Element Modelling of Roller Burnishing Process. *CIRP Annals - Manufacturing Technology* **2005**, *54* (1), 237–240.

3. Hassan, A.M.; Sulieman, Z.S. Improvement in the wear resistance of brass components by the ball burnishing process. *Journal of Materials Processing Technology* **1999**, *96*, 73–80.
4. Roettger, K. Walzen hartgedrehter Oberflaechen. PhD Dissertation, Werkzeugmaschinenlabor, RWTH Universität, Aachen, Germany, 2002.
5. López de la Calle, L.N.; Rodríguez, A.; Lamikiz, A.; Celaya, A.; Alberdi, R. Five-Axis Machining and Burnishing of Complex Parts for the Improvement of Surface Roughness. *Materials and Manufacturing Processes* **2011**, *26* (8), 997–1003.
6. Hassan, A.M. The effects of ball- and roller-burnishing on the surface roughness and hardness of some non-ferrous metals. *Journal of Materials Processing Technology* **1997**, *72*, 385–391.
7. El-Axir, M.H.; Othman, O.M.; Abodiena, A.M. Study on the inner surface finishing of aluminium alloy 2014 by ball-burnishing process. *Journal of Materials Processing Technology* **2008**, *202*, 435–442.
8. Travieso-Rodriguez, J.A.; Dessein, G.; Gonzalez-Rojas, H.A. Improving the Surface Finish of Concave and Convex Surfaces Using a Ball Burnishing Process. *Materials and Manufacturing Processes,* **2011**, *26* (12), 1494–1502.
9. Mech-India Engineers Pvt. Ltd. Retrieved from http://www.mechindia.com/. Last visited on 13/02/2014.
10. Ecoroll AG Werkzeugtechnik Hydrostatic Tools catalogue. Retrieved from http://www.ecoroll.de/en/products/hydrostatische-werkzeuge.html. Last visited on 13/02/2014.
11. Celaya, A.; Rodriguez, A.; Albizuri, J.; Lopez de la Calle, L.N.; Alberdi, R. Modelo de elementos finitos del bruñido. In *Proceedings of 9° Congreso Iberoamericano de Ingeniería Mecánica*, Las Palmas de G Canaria, Spain, 2009.
12. Rodriguez, A.; Lopez de la Calle, L.N.; Celaya, A.; Lamikiz, A.; Albizuri, J. Surface improvement of shafts by the deep ball-burnishing technique. *Surface & Coatings Technology* **2012**, *206*, 2817–2824.
13. Amini, S.; Paktinat, H.; Barani, A.; Fadaei Tehran, A. Vibration Drilling of Al2024-T6. *Materials and Manufacturing Processes* **2013**, *28* (4), 476–480.
14. Witthauera, A.T.; Kima, G.Y.; Faidleyb, L.E.; Zouc, Q.Z.; Wang, Z. Effects of Acoustic Softening and Hardening in High-Frequency Vibration-Assisted Punching of Aluminum. *Materials and Manufacturing Processes* **2014**, *29* (10), 1184–1189.
15. Travieso-Rodriguez, J.A.; Gonzalez-Rojas, H.A.; Casado-Lopez, R. Herramienta con bola a baja presión, aplicable para bruñido de superficies. *Spanish patent reference: P201130331. Boletín Oficial de la Propiedad Intelectual BOPI*, 21/11/ 2013.
16. Gomez-Gras, G.; Travieso-Rodriguez, J.A.; Gonzalez-Rojas, H.A.; Napoles-Alberro, A.; Carrillo, F.; Dessein, G. Study of a ball-burnishing vibration-assisted process. *Journal Trends in the Development of Machinery and Associated Technology,* **2013**, *17* (1), 49–53.
17. Travieso-Roriguez, J.A. Estudio para la mejora del acabado superficial de superficies complejas, aplicando un proceso de deformación plástica (Bruñido con Bola). PhD Thesis, Universitat Politècnica de Catalunya, Barcelona, Spain, 2010.
18. Noyan, I.C.; Cohen, J.B. *Residual stress. Measurements by diffraction and interpretation*; Springer-Verlag: New York, USA, 1987.
19. Hauk, V.M.; Macherauch, E. A useful guide for X-ray stress evaluation. *Advances in X-ray analysis,* **1983**, *26*, 81–99.
20. Kumar, A.; Welzel, U.; Mittermeyer, E.J. A method for the non-destructive analysis of gradients of mechanical stresses by X-ray diffraction measurements at fixed penetration/information depths. *Journal of Applied Cristalography* **2006**, *39* (5), 633–646.
21. Yen, Y.C.; Sartkulvanich, P.; Altan, T. Finite element modeling of roller burnishing process. *CIRP Annals - Manufacturing Technology* **2005**, *54* (1), 237–240.
22. Yin, S.; Shinmura, T. A comparative study: polishing characteristics and its mechanisms of three vibration modes in vibration-assisted magnetic abrasive polishing. *International Journal of Machine Tools & Manufacture* **2004**, *44*, 383–390.
23. Siegert, K.; Ulmer, J. Superimposing Ultrasonic Waves on the Dies in Tube and Wire Drawing. *Journal of Engineering Materials and Technology* **2001**, *123*, p 517.
24. Holstein, T. Theory of Ultrasonic Absorption in Metals: the Collision-Drag Effect. *Physical review* **1959**, *113* (2), 479–496.
25. Blaha, F.; Langenecker, B. Dehnung von Zink-Kristallen unter Ultraschalleinwirkung. *Naturwissenschaften* **1955**, *42* (20), p 556.
26. Zhang, Q.; Mahfouf, M.; Yates, J.R.; Pinna, C.; Panoutsos, G.; Boumaiza, S.; Greene, R.J.; de Leon, L. Modeling and Optimal Design of Machining-Induced Residual Stresses in Aluminium Alloys using a Fast Hierarchical Multiobjective Optimization Algorithm. *Materials and Manufacturing Processes* **2011**, *26* (3), 508–520.
27. El-Axis, M.M. An investigation into the ball burnishing of aluminium alloy 6061-T6. *Proceedings of the institution of mechanical engineers part B - Journal of engineering manufacture* **2007**, *221* (12), 1733–1742.